The αvβ6 integrin modulates airway hyperresponsiveness in mice by regulating intraepithelial mast cells

Kotaro Sugimoto,[1] Makoto Kudo,[1] Aparna Sundaram,[1] Xin Ren,[1] Katherine Huang,[1] Xin Bernstein,[1] Yanli Wang,[1] Wilfred W. Raymond,[2] David J. Erle,[1] Magnus Åbrink,[3] George H. Caughey,[2] Xiaozhu Huang,[1] and Dean Sheppard[1]

[1]Lung Biology Center, Department of Medicine, UCSF, San Francisco, California, USA. [2]Cardiovascular Research Institute, Department of Medicine, UCSF, Veterans Affairs Medical Center, San Francisco, California, USA. [3]Department of Biomedical Sciences and Veterinary Public Health, Swedish University of Agricultural Sciences, Biomedical Center, Uppsala, Sweden.

Allergic asthma is the most common form of asthma, affecting more than 10 million Americans. Although it is clear that mast cells have a key role in the pathogenesis of allergic asthma, the mechanisms by which they regulate airway narrowing in vivo remain to be elucidated. Here we report that mice lacking αvβ6 integrin are protected from exaggerated airway narrowing in a model of allergic asthma. Expression microarrays of the airway epithelium revealed mast cell proteases among the most prominent differentially expressed genes, with expression of mouse mast cell protease 1 (mMCP-1) induced by allergen challenge in WT mice and expression of mMCP-4, -5, and -6 increased at baseline in β6-deficient mice. These findings were most likely explained by loss of TGF-β activation, since the epithelial integrin αvβ6 is a critical activator of latent TGF-β, and in vitro–differentiated mast cells showed TGF-β–dependent expression of mMCP-1 and suppression of mMCP-4 and -6. In vitro, mMCP-1 increased contractility of murine tracheal rings, an effect that depended on intact airway epithelium, whereas mMCP-4 inhibited IL-13–induced epithelial-independent enhancement of contractility. These results suggest that intraepithelial activation of TGF-β by the αvβ6 integrin regulates airway responsiveness by modulating mast cell protease expression and that these proteases and their proteolytic substrates could be novel targets for improved treatment of allergic asthma.

Introduction

Mast cells are mainly known for their harmful effects during allergic inflammation and contribute to asthma in several ways (1). Mast cell activation induces degranulation and release of a range of inflammatory substances, including proteases, histamine, cytokines, chemokines, and lipid mediators. Proteases are the most conspicuous products of mast cells and mainly consist of chymases, tryptases, and carboxypeptidase A (CPA) (2). Mast cell degranulation is often seen in asthmatic lungs, and various mast cell mediators can be found in bronchoalveolar lavage (BAL) fluid from asthmatic patients. Infiltration of mast cells into the airway smooth muscle cell layer is a prominent feature of allergic asthma (3) and is associated with airway hyperresponsiveness (AHR) (4). Mice lacking functional mast cells are protected in models of asthma in which allergic airway inflammation is induced by administration of OVA without external adjuvant (5, 6). However, the precise mechanisms by which mast cells regulate airway narrowing in vivo remain to be determined.

The αvβ6 integrin is expressed in epithelial cells, where it plays an important role in activating latent TGF-β. Mice lacking this integrin are protected from pulmonary fibrosis (7, 8) and acute lung injury (9) and develop age-related emphysema (10), effects that all appear to be caused by a lack of active TGF-β. TGF-β is an important regulator of immune responses (11–13), but its role in asthma is controversial. TGF-β affects multiple processes involved in matrix remodeling in the lung (e.g., increased matrix production by fibroblasts, epithelial cell apoptosis, epithelial-mesenchymal transition, and modulation of protease secretion) (14–17) and directs the differentiation of Th17 cells, which can enhance allergic responses (11, 18, 19). On the other hand, TGF-β stimulates differentiation of regulatory T cells that can suppress allergic responses (11, 19, 20), and blocking TGF-β signaling specifically in T cells enhances airway hypersensitivity, airway inflammation, and Th2 cytokine production (21). Thus, in different contexts, TGF-β can either facilitate or inhibit allergic asthma.

Here we show that mice lacking the αvβ6 integrin were protected from AHR in a mast cell–dependent model of allergic asthma and demonstrate that this effect could be explained, at least in part, by specific effects of TGF-β on expression of mast cell proteases that either enhance (mMCP-1) or inhibit (mMCP-4) airway narrowing. mMCP-1 appeared to enhance airway smooth muscle contraction through effects on the epithelium, whereas the effect of mMCP-4 persisted in tracheal rings denuded of epithelium.

Results

β6-deficient mice are protected from AHR, but not from lung inflammation, mucus metaplasia, or airway remodeling. β6 KO and WT control mice on the same genetic background (FvB) were sensitized and challenged by intranasal administration of OVA or saline (as a control) using a regimen that was previously reported to depend on mast cells (5, 6). Airway responsiveness to acetylcholine was the same in saline-challenged WT and β6 KO mice, but β6 KO mice were

Authorship note: Kotaro Sugimoto and Makoto Kudo contributed equally to this work. Xiaozhu Huang and Dean Sheppard are co–senior authors.

Conflict of interest: The authors have declared that no conflict of interest exists.

Citation for this article: *J Clin Invest* doi:10.1172/JCI58815.

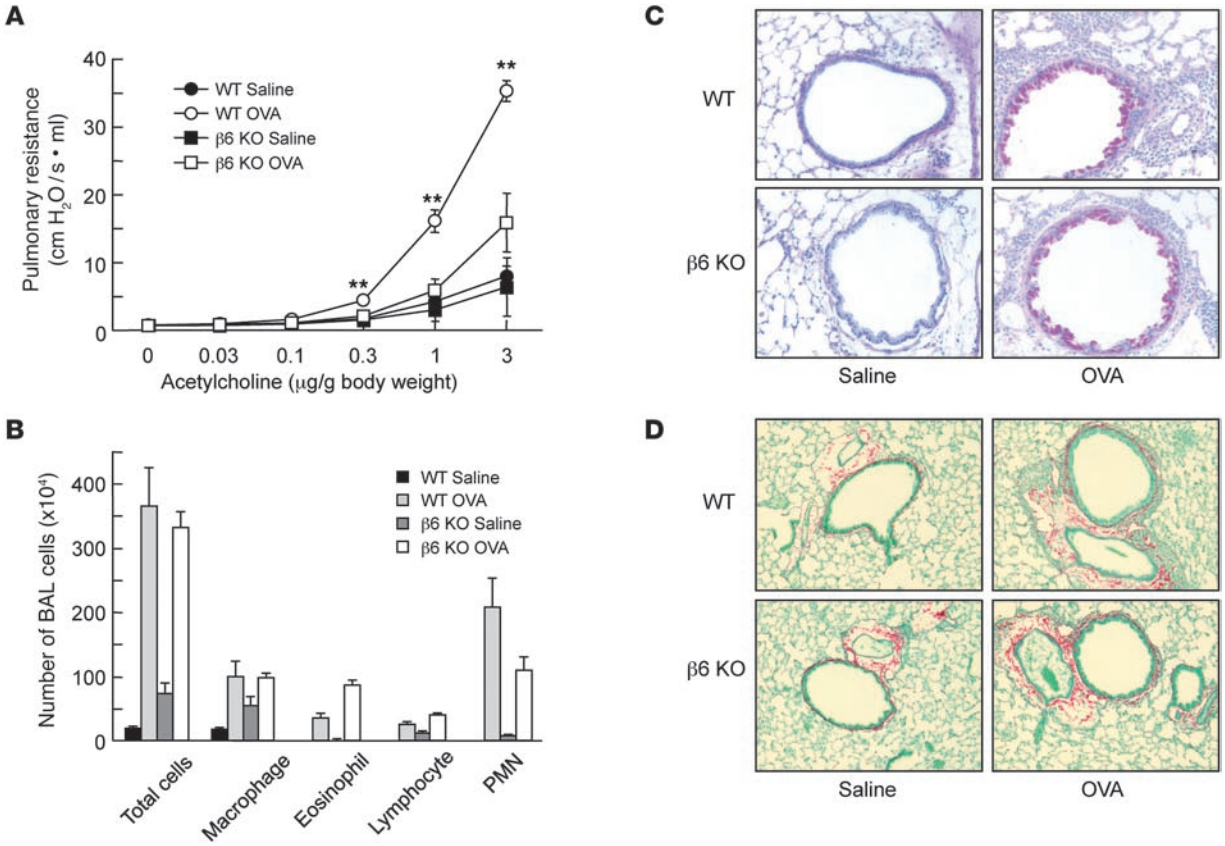

Figure 1

Protection of β6 KO mice from allergen-induced AHR, but not inflammation or remodeling. (**A**) Pulmonary resistance in response to a range of concentrations of intravenous acetylcholine in WT or β6 KO mice after sensitization and challenge with OVA or saline. Data are mean ± SEM; n = 6–9 per group. $^{**}P < 0.01$ vs. β6 KO OVA. (**B**) Counts for macrophages, eosinophils, lymphocytes, and polymorphonuclear leukocytes (PMN) in BAL fluid (n = 6–9). (**C**) Periodic acid–Schiff staining for mucus in representative lung sections. Magenta-staining epithelial cells are positive for mucus. Original magnification, ×200. (**D**) Sirius red staining for fibrosis in representative lung sections. Original magnification, ×100. Results are representative of at least 3 individual experiments.

significantly protected from increased AHR after OVA challenge (Figure 1A). In agreement with previous findings, saline-treated β6 KO mice had low-level baseline lung inflammation, but allergen-induced inflammation — detected by differential counting of cells obtained by BAL — did not differ between genotypes, nor did mucus metaplasia or subepithelial fibrosis (Figure 1, B–D). There was also no difference in the degree of sensitization, as determined by OVA-specific serum IgE (data not shown).

Design and characterization of a method to sample the airway epithelial microenvironment. To elucidate how loss of this epithelial integrin protects from AHR after allergen challenge, we developed a brushing method to specifically sample the airway epithelial microenvironment. This method harvested airway epithelium from central bronchi, and more than 90% of harvested cells were epithelial cells (Figure 2A). As determined by quantitative real-time RT-PCR (qRT-PCR), expression of 2 epithelial-restricted genes, *Cdh1* and *Foxj1* (encoding E-cadherin and FOXJ1, respectively), was well-represented in whole lung and brush-harvested epithelial samples, whereas 2 nonepithelial genes, *Acta2* and *Pecam1* (encoding α-SMA and PECAM-1, respectively), were largely absent only in airway brushing samples (Figure 2C), which confirmed that the samples obtained were highly enriched for airway epithelium.

Differential expression of mast cell genes in the airways of WT and β6 KO mice. Expression microarrays identified 119 genes that were significantly differentially expressed in WT and β6 KO mice after saline or chronic allergen challenge (adjusted $P < 0.05$; Figure 3A). Partitioning around mediods (PAM) clustering of the array data revealed 2 interesting clusters (referred to herein as clusters 1 and 2; Figure 3, B and C) that we had not identified in previous comparisons of whole lung microarrays. Cluster 1 consisted of 6 genes that were increased in saline-treated β6 KO mice; 5 of these encode mast cell proteases (*Cma1*, encoding mMCP-5; *Mcpt4*, encoding mMCP-4; *Cpa3*, encoding CPA3; *Mcpt6*, encoding mMCP-6; and *Tpsab1*, encoding mMCP-7), and the sixth, *Il1rl1* (encoding IL-33 receptor), is highly expressed in mast cells (22). These 6 transcripts were each among the most highly induced transcripts in saline-treated β6 KO mice compared with WT mice (Supplemental Table 1; supplemental material available online with this article; doi:10.1172/JCI58815DS1). The 11 genes of cluster 2 (*St6galnac2*, *Hs6st2*, *Fancd2*, *Spdef*, *Cd177*, *Flt3l*, *Mcpt1*, *Qscn6l1*, *Wnt5b*, *Itgae*, and *Mgam*) exhibited low expression at baseline in both WT and β6 KO mice and increased in WT mice, but not β6 KO mice, after chronic allergen challenge. The most highly induced gene in this cluster, *Mcpt1*, encodes another mast cell protease, mMCP-1, which

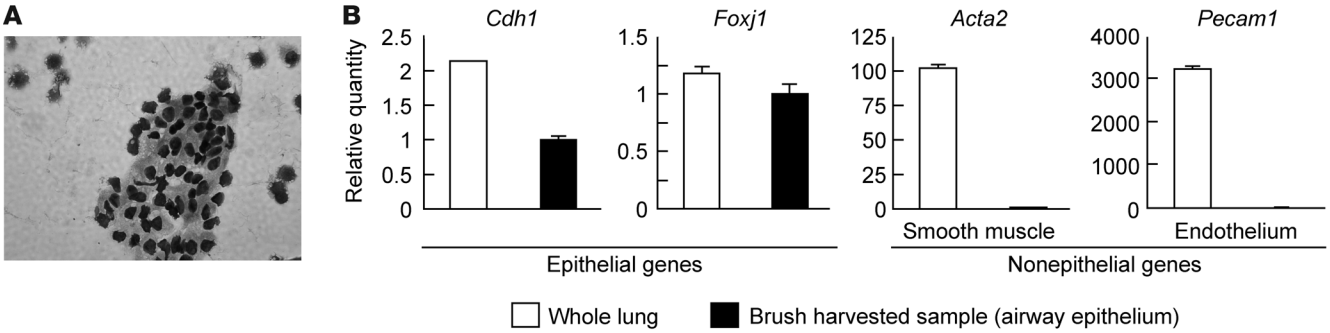

Figure 2

Characterization of a brush to sample murine airway epithelium. (**A**) HEMA 3 staining of brush-harvested airway epithelium. Original magnification, ×400. (**B**) qRT-PCR analysis of expression of epithelium-specific genes (*Cdh1* and *Foxj1*) and nonepithelial genes (*Acta2* and *Pecam1*) in whole lung and brush-harvested samples. Values for each mRNA were normalized to *Gapdh*, and relative quantity was calculated relative to expression in brush-harvested epithelium sample. Data are mean ± SEM for 3 independent samples.

was induced 18-fold in WT mice after allergen challenge, whereas none of the other genes were induced more than 2.5-fold. We also analyzed the most highly induced genes in WT mice after allergen challenge; of these, only *Mcpt1* was expressed at a significantly higher level in WT mice than in β6 KO mice (adjusted $P < 0.05$; Supplemental Table 2).

Thus, the most informative differentially expressed genes identified in microarrays of the epithelial microenvironment were not epithelial genes, but mast cell genes. We also could not find any substantial differential expression of cytokines, chemokines, or growth factors. To confirm these microarray findings of altered mast cell gene expression in brush-harvested airway epithelium, we reanalyzed samples by qRT-PCR (Figure 4A). We also analyzed the expression of the related mast cell gene *Mcpt2*, which encodes a proteolytically inactive gene product and is often coregulated with *Mcpt1*. Levels of *Mcpt1* and *Mcpt2* expression were low at baseline in epithelial samples from both WT and β6 KO mice and were significantly increased in WT mice, but not in β6 KO mice, after chronic allergen challenge. Expression of *Mcpt4*, *Mcpt5*, *Mcpt6*, and *Cpa3* transcripts were significantly increased at baseline in the β6 KO mice. As expected, in most cases, qRT-PCR gave a larger estimate of the magnitude of the increase in expression than did microarray, but the relative expression of each gene was similar by both methods. Importantly, none of these differences were apparent from qRT-PCR of RNA from whole lung (Supplemental Figure 1).

These results raised the possibility that mast cells might be more abundant, even in the absence of allergen challenge, within the epithelium of β6 KO mice. Cytospin preparation of brushing samples were stained for chloroacetate esterase activity to identify mast cells, and the ratio of mast cells to total cells was significantly increased in airway samples from β6 KO mice (Figure 4, B and C). The increase in intraepithelial mast cells was confirmed by toluidine blue staining of tracheal sections from unchallenged mice, with mast cell numbers increased 7-fold in the epithelium of β6 KO mice (Figure 4, D and E).

The increase in the number of intraepithelial mast cells at baseline in β6 KO mice likely contributed to the increase in *Mcpt4*, *Mcpt5*, *Mcpt6*, and *Cpa3* seen in epithelial brushings from these animals. To determine whether the increase in mast cell number was the sole cause of these changes in gene expression, we normalized the gene expression level for number of intraepithelial mast cells. After normalization, the levels of *Mcpt4*, *Mcpt5*, *Mcpt6*, and *Cpa3* remained significantly higher in untreated β6 KO mice than in WT control mice (Supplemental Figure 2), which suggests that both increased mast cell numbers and changes in gene expression in each mast cell likely contribute to the overall increase observed in the expression of these mast cell protease genes.

TGF-β directly regulates mast cell protease expression. mMCP-1 and mMCP-2 have previously been shown to be induced by TGF-β (23, 24), but previous studies have not described effects of TGF-β on mMCP-4, mMCP-5, mMCP-6, or CPA3. We thus evaluated whether TGF-β might fully explain differences in mast cell protease expression in β6 KO mice by differentiating BM-derived cultured mast cells (BMCMCs) in the presence or absence of TGF-β. After 3 weeks of culture, qRT-PCR analyses revealed TGF-β–dependent induction of *Mcpt1* (171-fold) and *Mcpt2* (47-fold) and suppression of *Mcpt4* (11-fold) and *Mcpt6* (6-fold) (Figure 5A). Expression of *Mcpt5* and *Cpa3* (data not shown) was not affected by TGF-β. Western blotting of BMCMC lysates confirmed that TGF-β induced the expression of mMCP-1 and mMCP-2 and suppressed the expression of mMCP-4 and mMCP-6 (Figure 5B). BMCMCs from β6 KO mice secreted comparable levels of mMCP-1 when differentiated in the presence of recombinant TGF-β and secreted comparable levels of mMCP-6 when differentiated in the absence of recombinant TGF-β to WT BMCMCs (Supplemental Figure 4), which suggests that the differences we observed in vivo are not caused by unresponsiveness of mast cells in these mice to active TGF-β. Although the recombinant TGF-β–induced increase in *Mcpt1* mRNA appeared to be reduced in BMCMCs from β6 KO mice, recombinant TGF-β still increased mMCP-1 expression by more than 100-fold. Together with comparable induction of mMCP-1 protein secretion, these observations lead us to believe that this apparent difference is unlikely to have biological meaning.

mMCP-1 directly enhances murine tracheal contractility. To determine whether differences in mast cell protease expression could explain the protection of β6 KO mice from allergen-induced AHR, we evaluated effects of supernatants from activated BMCMCs differentiated in the presence or absence of TGF-β on the contractility of mouse tracheal rings. Degranulation in response to DNP-IgE and DNP was similar in both types of BMCMCs, as determined by β-hexosaminidase release (Figure 5C), and TGF-β did not differentially affect mast cell numbers, as determined by flow cytometry

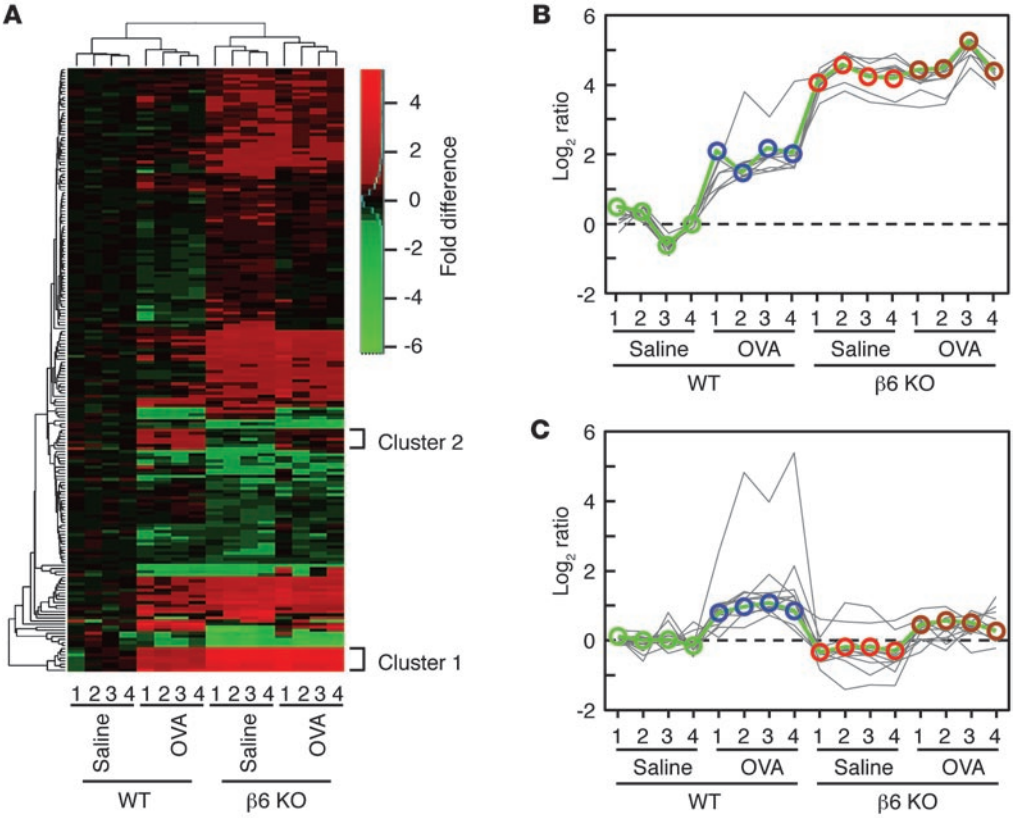

Figure 3

Global analysis of gene expression in airway samples from saline- or OVA-challenged WT and β6 KO mice. (**A**) Heat map of the array results. Each column represents data from 1 of 4 replicate samples per group. Colors represent fold differences of $\log_2$ expression ratios compared with epithelial cells from saline-treated WT mice. (**B**) Cluster 1 (8 oligonucleotide probes for a total of 6 genes) from PAM clustering. (**C**) Cluster 2 (11 genes) from PAM clustering.

with *c*-kit antibody (data not shown). mMCP-1 was only detected in the supernatant of activated BMCMCs differentiated in the presence of TGF-β, and mMCP-6 was only detected from BMCMCs differentiated in the absence of TGF-β (Figure 5D). mMCP-2 was also detected in the supernatant in which TGF-β was present, but mMCP-4 was not detected in the supernatant lacking TGF-β (data not shown), perhaps because of low sensitivity of the only available antibody to mMCP4. We added supernatants to tracheal rings and assessed contractile responses after 30-minute incubations (Figure 6A). Whereas supernatant lacking TGF-β had no effect on methacholine-induced contraction, supernatant containing TGF-β significantly increased responses to methacholine. To determine the role of proteases in this response, we added various protease inhibitors to the supernatants (Figure 6B). Only the chymotrypsin inhibitor chymostatin, an effective inhibitor of mast cell chymases (25), inhibited enhanced contractility, whereas the cysteine and trypsin-like protease inhibitor leupeptin and the metalloprotease inhibitor marimastat did not. Supernatant with TGF-β contained 2 chymase family members, mMCP-1 and mMCP-2 (Figure 5D), but mMCP-2 does not have protease activity (23). To determine whether enhancement of airway contractility was induced specifically by mMCP-1, we evaluated the effects of TGF-β–containing supernatant from mMCP-1 KO mice (Figure 6C). The absence of *Mcpt1* transcripts in BMCMCs derived from mMCP-1 KO mice was confirmed by qRT-PCR (Supplemental Figure 3A). Supernatants from mMCP-1 KO BMCMCs were completely devoid of contractility-enhancing activity. Moreover, direct incubation of activated recombinant mMCP-1 (rmMCP-1) with tracheal rings enhanced methacholine-induced contractility to the same extent as did WT mouse supernatant with TGF-β (Figure 6, C and D).

mMCP-4 suppresses IL-13–induced murine tracheal contractility. β6 KO mice have increased numbers of intraepithelial mast cells at baseline that specifically express mMCP-4 and mMCP-6. Given the protection of these mice from AHR induced by allergen challenge, we wondered whether these proteases specifically inhibit allergen challenge–induced enhanced airway smooth muscle contractility. One of the central mediators of allergen-induced AHR is IL-13, which has previously been shown to directly increase contractility of tracheal rings (26). We therefore incubated tracheal rings for 12 hours with either IL-13 or saline, washed out the cytokine, and then examined the effects of 30-minute incubation with supernatants of degranulated BMCMCs from WT mice (Figure 7A). As expected, IL-13 enhanced methacholine-induced contraction, and this augmented contractility was significantly inhibited by supernatant in which TGF-β was absent. This suppressive effect was significantly inhibited by chymostatin, but not by other protease inhibitors with less effect on chymases (Figure 7B). Supernatant lacking TGF-β contained a single chymase (mMCP-4), 1 elastase (mMCP-5), 2 tryptases (mMCP-6 and mMCP-7), and a metalloexopeptidase (CPA3). Our finding that chymostatin, but not leu-

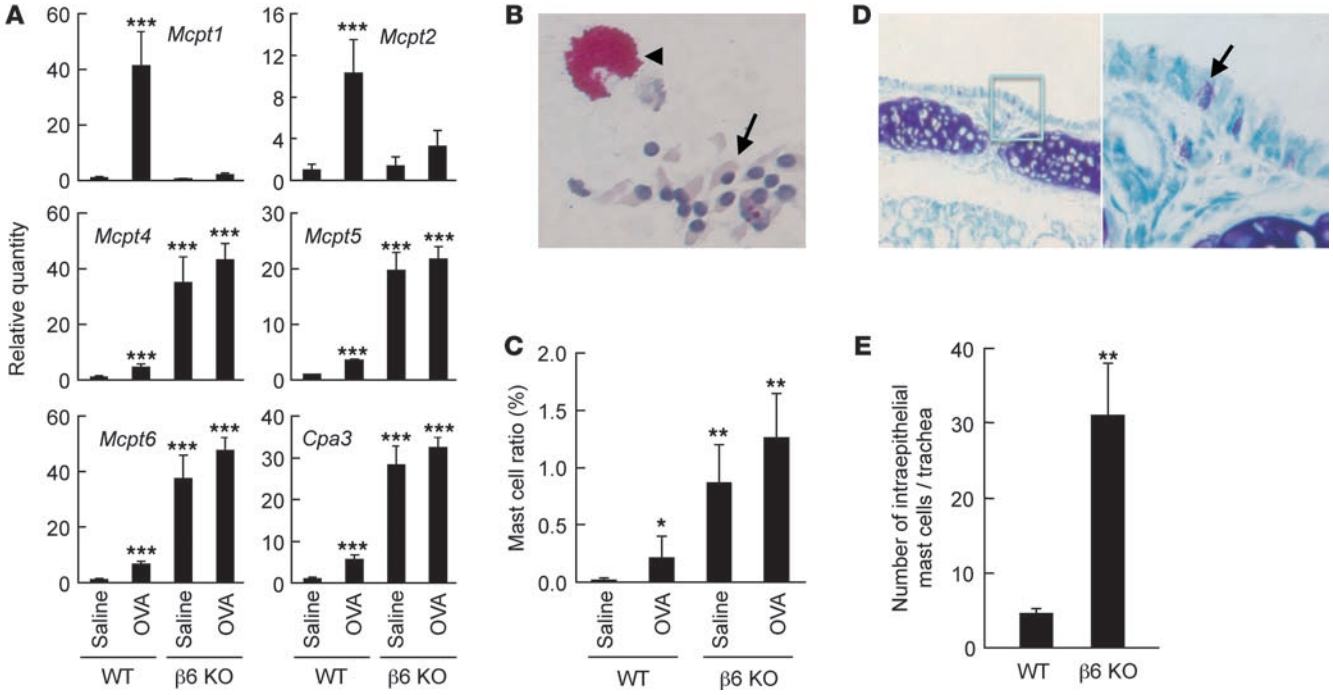

Figure 4

Differential expression of mast cell transcripts and mast cell number in the airway epithelium of allergen-challenged WT and β6 KO mice. (**A**) qRT-PCR of mast cell protease transcripts identified by microarray analysis. Epithelial RNA was harvested from saline- or allergen-challenged mice, reverse transcribed, and amplified by qRT-PCR. Values for each mRNA were normalized to *Gapdh*, and relative quantity was calculated relative to expression in saline-treated WT mice. Data are mean ± SEM for 5 independent samples. ***$P < 0.001$ vs. WT saline. (**B**) Example of epithelial cell (arrow) and mast cell (arrowhead) identified from cytospin preparation of brushing samples via chymase-like chloroacetate esterase activity. Sample is from an untreated β6 KO mouse. Original magnification, ×400. (**C**) Mast cell ratios in cytospin preparations of epithelial samples. Ratios were calculated by counting cells under light microscopy. Data are mean ± SEM; n = 4–5 per group. *$P < 0.05$, **$P < 0.01$ vs. WT saline. (**D**) Section of mouse trachea obtained from untreated β6 KO mouse stained with toluidine blue. Arrow denotes mast cell. Higher-magnification view of the boxed region is also shown. Original magnification, ×100 (left), ×400 (right). (**E**) Intraepithelial mast cell number in tracheal sections. Data are mean ± SEM; n = 4–5 per group. **$P < 0.01$ vs. WT.

peptin or marimastat, blocked this protective effect suggested it might be caused by mMCP-4. We thus differentiated BMCMCs from mMCP-4 KO mice, confirmed the absence of *Mcpt4* by qRT-PCR (Supplemental Figure 3B), and found that supernatants from BMCMCs derived from mMCP-4 KO mice were completely devoid of this suppressive activity (Figure 7A). Activated rmMCP-4 also significantly suppressed IL-13–induced enhancement of contractility, without effects on baseline responses (Figure 7C). In mice, there are several expressed mast cell chymase-like proteases, but there is only 1 chymase in humans, and its functional homolog is thought to be mMCP-4 (27). We therefore evaluated the effect of recombinant human chymase on IL-13–enhanced contraction and found significant suppression, similar to the effects of rmMCP-4 (Figure 7, C and D).

Enhanced tracheal ring contractility by mMCP-1 is epithelium dependent, and suppression of IL-13–induced tracheal contractility by mMCP-4 is epithelium independent. Tracheal rings include a number of cell types, including a layer of epithelial cells. To evaluate whether mast cell products act directly on epithelial cells, we removed epithelium from tracheal rings (Figure 8A) and examined the effects of mMCP-1 and mMCP-4 on contraction. As expected, epithelium removal enhanced the magnitude of force generation in response to methacholine. In tracheal rings with epithelium removed, supernatant in which TGF-β was present was completely devoid of contractility-enhancing activity, and a similar effect was seen for activated rmMCP-1 (Figure 8, B and C). In contrast, supernatants of mast cells differentiated in the absence of TGF-β significantly suppressed IL-13–induced contractility in rings that were completely denuded of epithelium, and a similar effect was seen for rmMCP-4 (Figure 8, D and E).

Discussion

TGF-β has been previously shown to exert pleiotropic, context-specific effects on allergic asthma, mostly through effects on T cells, fibroblasts, and potentially smooth muscle cells (14, 18–21, 28). Our findings suggest novel roles for TGF-β as a potent switch regulating mast cell protease expression and as an inhibitor of mast cell accumulation within the airway epithelium. These effects appear to play an important role in regulating contractile responses of airway smooth muscle and in vivo AHR after chronic allergen challenge. Previous studies using mast cell–deficient mice have shown that mast cells contribute to AHR development when mice are sensitized and challenged with an adjuvant-free regimen (5, 6), as we used here. Our results suggest that these effects are probably caused by TGF-β–dependent differentiation of intraepithelial mast cells expressing mMCP-1, but not those expressing mMCP-4. Our

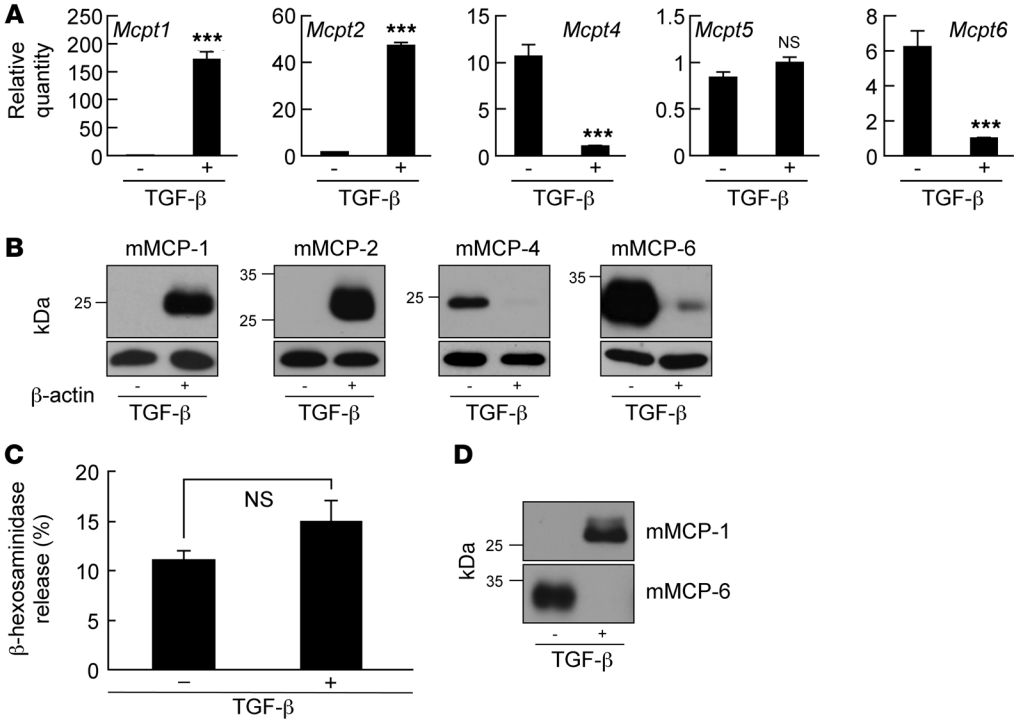

Figure 5

Characterization of mouse BMCMCs differentiated in the presence or absence of TGF-β. (**A**) Expression profiles of mast cell protease transcripts in cultured BMCMCs differentiated in the presence (+) or absence (–) of TGF-β for 3 weeks. mRNA concentrations were determined by qRT-PCR and normalized to *Gapdh*. *Mcpt1* and *Mcpt2* quantity was calculated relative to expression in samples lacking TGF-β, and *Mcpt4*, *Mcpt5*, and *Mcpt6* quantity was calculated relative to expression in samples with TGF-β. Data are mean ± SEM for 3 independent samples measured in triplicate. ***$P < 0.001$ vs. no TGF-β. (**B**) Western blot analysis of mast cell proteases in 2 μg protein from cell lysates of cultured BMCMCs differentiated in the presence or absence of TGF-β. β-actin was used as a control for equal protein loading. (**C**) Degranulation of BMCMCs differentiated in the presence or absence of TGF-β, assessed by β-hexosaminidase release after 24 hours incubation with anti–DNP-IgE followed by 1 hour stimulation with DNP-BSA. (**D**) Western blot analysis of mast cell proteases in the supernatant of degranulated BMCMCs.

results also suggest that mast cell–dependent induction of AHR might be prevented by inhibition of the αvβ6 integrin within the airway epithelium.

Although previous work suggested that expression of mMCP-1 and mMCP-2 in intestinal intraepithelial mast cells depends on TGF-β activation through the αvβ6 integrin and that TGF-β is required for differentiation of mMCP-1– and mMCP-2–expressing mast cells in vitro (23), to our knowledge, our finding that mMCP-4 and mMCP-6 expression was inhibited by TGF-β is novel. We were also surprised to find significant accumulation of mMCP-4– and mMCP-6–containing mast cells within the epithelium in the absence of αvβ6-mediated TGF-β activation. Previous studies of intraepithelial mast cells in the intestinal epithelium of β6 KO mice identified mast cells by mMCP-1 immunostaining (29), and might thus have missed these intraepithelial mast cells that do not express mMCP-1. In the present study, we did not determine the mechanisms that lead to accumulation of these mast cells in the absence of local TGF-β activation. TGF-β has been reported to promote mast cell proliferation and migration (30). Mitogen-activated protein kinase activity and integrins have previously been shown to be involved in TGF-β–regulated mast cell migration (31–33). However, TGF-β1 has also been reported to act as a negative regulator of mast cell function (34), and it is well accepted that mast cell proliferation and migration can be regulated by different mechanisms in different locations (35). Mast cells are also known to accumulate at sites of inflammation (36), so it is possible that the increase in baseline intraepithelial mast cells in β6 KO mice is caused by their low-level baseline inflammation, as we have previously described (37).

It is noteworthy that the significant differences in intraepithelial mast cell numbers and mast cell protease expression we describe here were not at all apparent from microarray or qRT-PCR analysis of whole lung samples. These effects could only be identified by sampling the airway epithelial microenvironment. The simple airway brush we have developed should thus be a useful tool for future investigations of cellular and gene expression changes that are restricted to the epithelium.

The protective effects of mMCP-4 on airway smooth muscle contractility were somewhat surprising, given the extensive literature describing the contributions of mast cells to the pathophysiology of allergic asthma and AHR (1, 4, 5, 38, 39). However, our findings are consistent with a previous report of enhanced AHR after allergen challenge in mice lacking mMCP-4 (40). Furthermore, mMCP-4 is the closest functional homolog of human mast cell chymase (27), and epithelial chymase expression has been suggested to be protective against asthma severity in human subjects with asthma

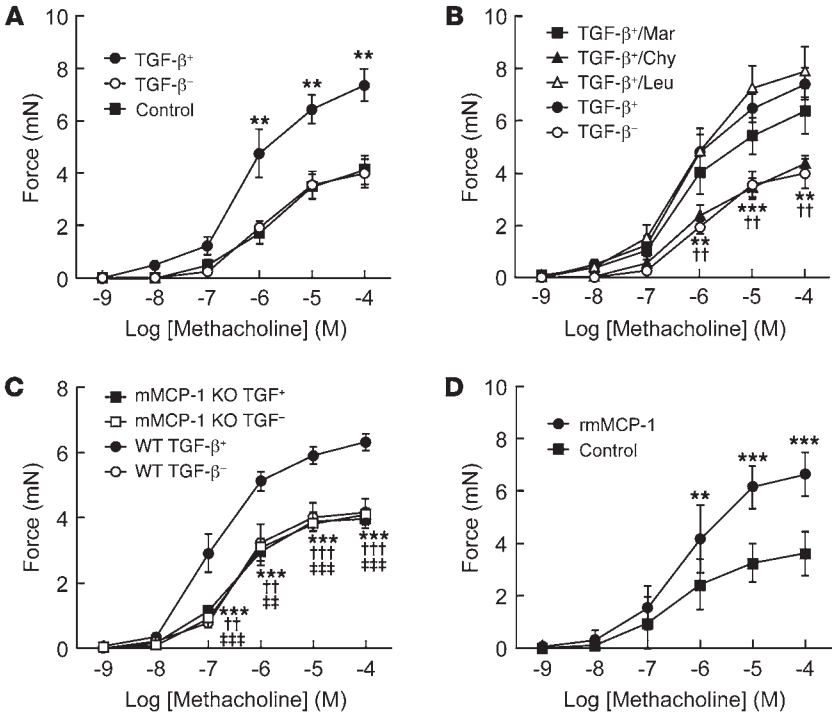

Figure 6

mMCP-1 enhances in vitro contractility of murine tracheal rings. (**A**) Tracheal rings (n = 6 per group) were incubated with the supernatant of degranulated BMCMCs differentiated in the presence or absence of TGF-β (TGF-β$^+$ and TGF-β$^-$, respectively) before assessment of contractility to methacholine. $^{**}P < 0.01$ vs. control. (**B**) Supernatant of degranulated BMCMCs were incubated with 1 μM marimastat (Mar), 10 μg/ml chymostatin (Chy), or 10 μg/ml leupeptin (Leu) for 15 minutes at room temperature, followed by incubation with tracheal rings (n = 6–7 per group) before assessment of contractility to methacholine. $^{**}P < 0.01$, TGF-β$^+$/Chy vs. TGF-β$^+$; $^{††}P < 0.01$, TGF-β$^+$ vs. TGF-β$^-$. (**C**) Supernatant from degranulated BMCMCs from WT or mMCP-1 KO mice was added to tracheal rings (n = 6 per group) as in **A**. $^{**}P < 0.01$, $^{***}P < 0.001$, WT TGF-β$^-$ vs. WT TGF-β$^+$; $^{††}P < 0.01$, $^{†††}P < 0.001$, mMCP-1 KO TGF-β$^-$ vs. WT TGF-β$^+$; $^{‡‡}P < 0.01$, $^{‡‡‡}P < 0.001$, mMCP-1 KO TGF-β$^+$ vs. WT TGF-β$^+$. (**D**) rmMCP-1 was activated by cathepsin C, and tracheal rings (n = 12 per group) were treated with active rmMCP-1 (6 ng/μl) and followed by assessment of contractility to methacholine. $^{**}P < 0.01$, $^{***}P < 0.001$ vs. control. All data are mean ± SEM.

(41, 42). Given the increased number of intraepithelial mast cells we observed in β6 KO mice, it seems likely that the increased levels of *Mcpt4* and *Mcpt6* we observed were caused by the combined effects of increased mast cell accumulation and increased *Mcpt4* and *Mcpt6* expression in these cells.

Interestingly, mMCP-1 and mMCP-4 not only exert opposite effects on airway contractility, they do so by acting on distinct cell types. Our observation that the contractility-enhancing effect of mMCP-1 was completely abrogated by removal of airway epithelium suggests that mMCP-1 is released within the epithelium and acts directly on a substrate within the epithelial compartment to enhance airway smooth muscle contraction and airway narrowing. In contrast, the inhibitory effects of mMCP-4 on IL-13–enhanced airway contractility were completely preserved in tracheal rings denuded of epithelium, which suggests that mMCP-4 is acting on substrates outside of the epithelial compartment. One attractive hypothesis is that mMCP-4 acts directly on substrates on airway smooth muscle cells. However, given the cellular complexity of tracheal rings, the evidence presented here cannot exclude effects on substrates on other cells or extracellular compartments in the airway wall.

One obvious issue not addressed by the current work is the precise nature of the proteolytic substrates for mMCP-1 and mMCP-4 that regulate the opposing effects of these proteases on airway smooth muscle contractility. Although not much is known about substrates for mMCP-1, several substrates have been described for mMCP-4, including angiotensin I, pro-gelatinase, hepatocyte growth factor, thrombin, and fibronectin (27, 43–46). However, the in vivo relevance of these substrates to airway responsiveness is unclear. Identification of the substrates responsible for the effects described herein could lead to new strategies for protection against AHR and human asthma. Although there is no precise human ortholog for mMCP-1, once the proteolytic substrate and downstream molecular cascade responsible for enhancement of airway smooth muscle contractility is identified, the potential relevance of this pathway to human asthma could be more readily evaluated.

Methods

Reagents. Rat anti–mMCP-1 monoclonal antibody (RF6.1) (47) and sheep anti–mMCP-2 polyclonal antibody (23) were provided by A. Pemberton (University of Edinburgh, Edinburgh, United Kingdom). Goat anti–mMCP-4 polyclonal antibody and rat anti–mMCP-6 monoclonal antibody were purchased from Abcam and R&D, respectively. Mouse anti–β-actin monoclonal antibody was purchased from Abcam. Marimastat, chymostatin, and leupeptin were from Tocris, Sigma-Aldrich, and Roche, respectively. Recombinant pro–mMCP-1 was purchased from R&D and activated by recombinant mouse active cathepsin C/DPPI (R&D). rmMCP-4 was expressed by ligation-independent cloning of the catalytic domain cDNA into the pIEx 3 insect expression vector (Novagen), which encodes an N-terminal signal/pseudopropeptide incorporating glutathione S-transferase, the S-Tag sequence, a poly-His segment for use in nickel affinity purification, and an enteropeptidase cleavage site immediately preceding the catalytic domain sequence. Expression of the full-length chimera resulted in precipitation of the recombinant preprotein, which was resolved by reengineering the pseudopropeptide by replacing the portion of the expression plasmid encoding glutathione S-transferase with a short linker sequence encoding the amino acid sequence PERWA. The plasmid was transfected into Sf-9 insect cells grown in serum-free media. Recombinant protein was partially purified by heparin chromatography, activated by digestion with enteropeptidase, and further purified by cation exchange chromatography, which separated active mMCP-4 from enteropeptidase. Recombinant human pro-chymase was expressed, activated, and purified as described previously (48).

Mice. Mice functionally deficient in β6 integrin have been previously characterized (37). All of the experiments using β6 KO mice were con-

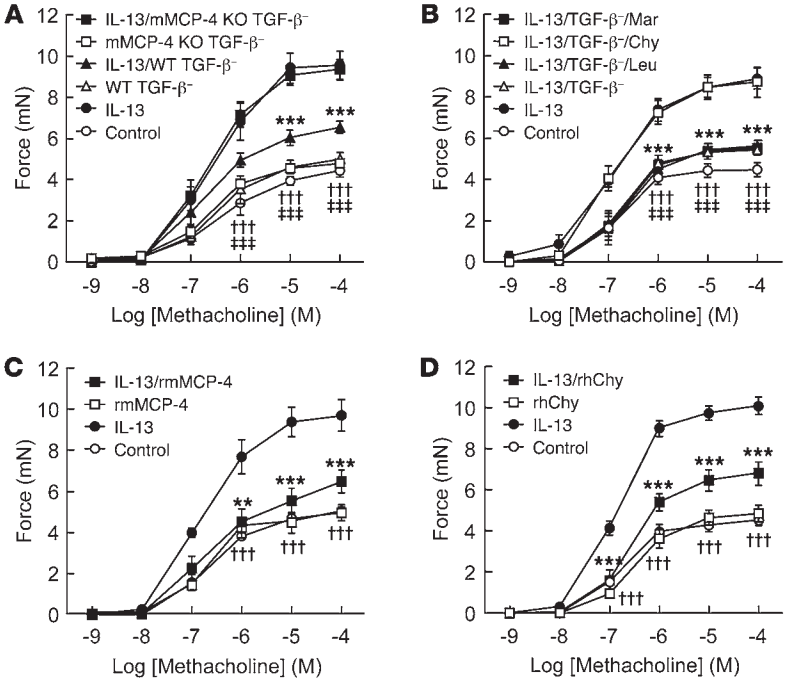

Figure 7

mMCP-4 suppresses IL-13–induced enhancement of tracheal contractility. (**A**) Tracheal rings (n = 6 per group) were treated with IL-13, washed, and incubated with the supernatant of degranulated BMCMCs from WT or mMCP-4 KO mice differentiated in the absence of TGF-β before assessment of contractility to methacholine. ***P < 0.001, IL-13/WT TGF-β⁻ vs. IL-13; †††P < 0.001, mMCP-4 KO TGF-β⁻ vs. IL-13; ‡‡‡P < 0.001, WT TGF-β⁻ vs. IL-13. (**B**) Supernatant of degranulated BMCMCs from WT mice were incubated with 1 μM marimastat, 10 μg/ml chymostatin, or 10 μg/ml leupeptin for 15 minutes at room temperature, followed by incubation with tracheal rings pretreated with IL-13 (n = 6 per group) as in **A** before assessment of contractility to methacholine. ***P < 0.001, IL-13/TGF-β⁻ vs. IL-13 and IL-13/TGF-β⁻/Chy, †††P < 0.001, IL-13/TGF-β⁻/Mar vs. IL-13 and IL-13/TGF-β⁻/Chy; ‡‡‡P < 0.001, IL-13/TGF-β⁻/Leu vs. IL-13 and IL-13/TGF-β⁻/Chy. (**C**) Tracheal rings (n = 6 per group) were treated with IL-13, washed, and incubated with active rmMCP-4 (1.4 ng/μl) before assessment of contractility to methacholine. **P < 0.01, ***P < 0.001, IL-13/rmMCP-4 vs. IL-13; †††P < 0.001, rmMCP-4 vs. IL-13. (**D**) Active recombinant human chymase (rhChy; 1.7 ng/μl) was incubated with tracheal rings (n = 6 per group) as in **C**. ***P < 0.001, IL-13/rhChy vs. IL-13; †††P < 0.001, rhChy vs. IL-13. All data are mean ± SEM.

ducted in mice backcrossed 5–10 generations to FVB/NJ background. mMCP-4 KO mice have been previously described (49). mMCP-1 KO mice were purchased from the mutant mouse regional resource center at University of Missouri. Mice used for all the experiments were 6–8 weeks old and housed under specific pathogen–free conditions in the Animal Barrier Facility of UCSF.

Sensitization and challenge. Mice were sensitized on days 1, 4, and 7 by intraperitoneal injection of 10 μg OVA in a total volume of 200 μl saline. Control animals received an equal volume of saline only. Mice were lightly anesthetized with isoflurane inhalation and intranasally challenged with OVA (20 μg in 30 μl saline) or saline every 7 days during days 14–70.

Measurement of airway response to acetylcholine. 24 hours after the last challenge, pulmonary resistance was measured in response to a range of concentrations of intravenous acetylcholine using the forced oscillation technique with the FlexiVent system (SCIREQ) as previously described (50).

Assessment of pulmonary inflammation and mucus production. Total and differential cell percentages were determined by counting in a hemocytometer and by light microscopic evaluation of more than 300 cells per slide as previously described (50). After lavage, lungs were inflated with 10% buffered formalin to 25 cm H_2O and transferred to 10% buffered formalin. 5-μm sections were stained with H&E for morphology, periodic acid–Schiff reagent for evaluation of mucus production, and Sirius red for evaluation of fibrosis.

Brushing method for harvesting murine airway epithelium. Brushes were made from 60-grit sandpaper–polished polyethylene PE-10 tube (BD Biosciences) with an inserted stainless wire (0.095 mm diameter). For epithelial harvesting, mice were anesthetized with ketamine (100 mg/kg body weight) and xylazine (10 mg/kg), the brush was inserted through an incision into the midsection of the trachea, and harvested epithelium was collected into 400 μl phosphate-buffered saline for cytospin preparation or 350 μl RNeasy lysis buffer (Buffer RLT; Qiagen) for RNA preparation. Cytospin cells were stained with a HEMA 3 stain set (Fisher) for checking the morphology of epithelium and with naphthol AS-D chloroacetate esterase staining kit (Sigma-Aldrich) for mast cells according to the manufacturer's instructions. For counting intraepithelial mast cell numbers in murine trachea, tracheas were fixed in 10% formalin for 48 hours and embedded in paraffin. 5-μm sections were stained with 0.5% toluidine blue (Sigma-Aldrich) in 0.5 M HCl.

Expression microarray analysis. 24 hours after the last challenge, airway epithelium was brush-harvested, and RNA quality was confirmed by Agilent nanotechnology. Expression microarrays were performed using Agilent Bioanalyzer (Mouse One-Color 4x44K array platform) in the UCSF Sandler Asthma Basic Research Center Functional Genomics Core Facility. Additional information about microarray protocols and complete microarray data are available from Gene Expression Omnibus (accession no. GSE28168; http://www.ncbi.nlm.nih.gov/geo/query/acc.cgi?acc=GSE28168).

BMCMC culture. BMCMC culture was performed as described previously (51), with a slight modification. Briefly, BM cells prepared from femurs of 10- to 12-week-old sex-matched mice were cultured for 21 days in DMEM supplemented with 10% fetal bovine serum, 100 U/ml penicillin, 100 μg/ml streptomycin, 2.5 μg/ml fungizone, 2 mM L-glutamine, and 1 mM sodium pyruvate. Mast cell growth and differentiation were stimulated with mouse IL-3 (1 ng/ml; R&D), mouse IL-9 (5 ng/ml; R&D), and mouse stem cell factor (50 ng/ml; PeproTech) with or without human TGF-β1 (1 ng/ml; R&D).

BMCMC degranulation. After 3 weeks of culture, BMCMCs (1×10^6 cells/ml) were sensitized with 1 μg/ml anti–DNP-IgE mAb (SPE7; Sigma-Aldrich) overnight at 37°C, washed, and resuspended at 2.5×10^5 cells/ml in Tyrode buffer (12 mM $NaHCO_3$, 0.4 mM NaH_2PO_4, 137 mM NaCl, 2.7 mM KCl, 1.8 mM $CaCl_2$, 1 mM $MgCl_2$, 5.6 mM D-glucose, and 0.1% BSA [pH 7.4]). Degranulation was initiated by addition of 10 ng/ml DNP-BSA (Invitrogen) for 30 minutes at 37°C. The degree of degranulation was determined by release of β-hexosaminidase (52). The remaining cells were lysed by addition with Tyrode buffer containing 0.1% Triton X-100. The supernatants and cell lysates (20 μl each) were incubated with 80 μl of 2.9 mM 4-nitrophenyl-*N*-acetyl-β-D-glucosa-

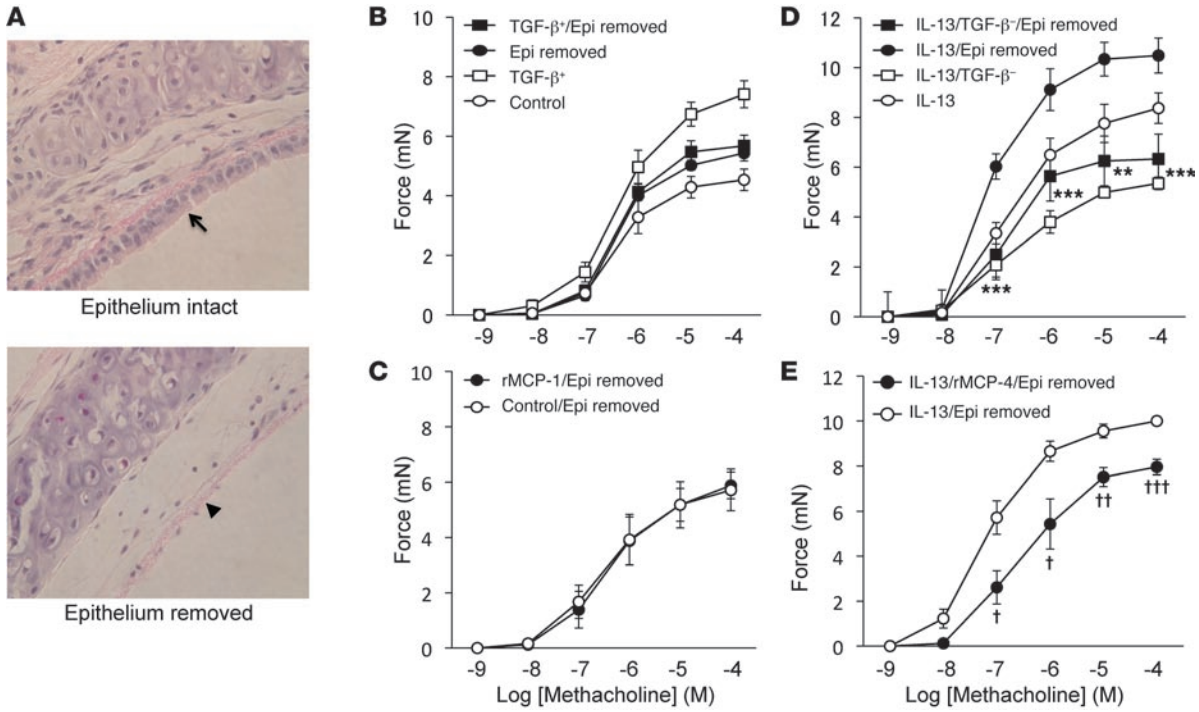

Figure 8

Enhanced tracheal ring contractility by mMCP-1 is epithelium dependent, and suppression of IL-13–induced tracheal contractility by mMCP-4 is the direct effect on smooth muscle. (**A**) H&E-stained sections from tracheal rings with epithelium intact (arrow) or removed (arrowhead). Original magnification, ×400. (**B** and **C**) Tracheal rings with epithelium intact or removed (n = 6 per group) were incubated with the supernatant of degranulated BMCMCs differentiated in the presence of TGF-β (**B**) or with rmMCP-1 (**C**) before assessment of contractility to methacholine. (**D** and **E**) Tracheal rings with epithelium intact or removed (n = 6 per group) were treated with IL-13, washed, and incubated with the supernatant of degranulated BMCMCs from WT mice differentiated in the absence of TGF-β (**D**) or with rmMCP-4 (**E**) before assessment of contractility to methacholine. $^{**}P < 0.01$, $^{***}P < 0.001$, IL-13/TGF-β$^-$ vs. IL-13/epithelium removed; $^{\dagger}P < 0.05$, $^{\dagger\dagger}P < 0.01$, $^{\dagger\dagger\dagger}P < 0.001$, IL-13/rMCP-4/epithelium removed vs. IL-13/epithelium removed.

minide (Sigma-Aldrich) in 0.1 M sodium citrate buffer (pH 4.8) for 1 hour at 37°C. The reaction was terminated by the addition of 200 μl 0.1 M sodium carbonate buffer (pH 10.2). The release of the product 4-nitrophenol was detected by measuring absorbance at 405 nm. Controls without antigen were used to measure spontaneous release. Release in the supernatant was calculated as percent total cellular (lysate plus supernatant) β-hexosaminidase.

Measurement of tracheal smooth muscle contractility. Tracheal ring segments approximately 3 mm in length were suspended in a 15-ml organ bath by 2 stainless steel wires (0.2 mm diameter) passed through the lumen. One wire was fixed to the organ bath, while the other was connected to a force-displacement transducer (FT03; Grass Instrument Co.) for the measurement of isometric force. A resting tension of 0.5 g was applied, and rings were equilibrated for 45 minutes. The buffer solution containing modified Krebs-Henseleit solution (117.5 mM NaCl, 5.6 mM KCl, 2.5 mM $CaCl_2$, 1.18 mM $MgSO_4$, 25 mM $NaHCO_3$, 1.28 mM NaH_2PO_4, and 5.55 mM glucose) was maintained at 37°C and oxygenated with 95% O_2, 5% CO_2. After incubation with the supernatant of degranulated BMCMCs (30 μl/ml final concentration) for 30 minutes at 37°C, rings were initially contracted in response to 60 mM KCl, and only rings that could generate more than 2.5 mN tension were used for experiments. Contractile response was evaluated with increasing concentrations of methacholine (10^{-9} to 10^{-4} M). For analysis of suppressive effects on IL-13–induced contractility, rings were treated with IL-13 (100 ng/ml; Peprotech) in DMEM, 10 mM HEPES (pH 7.3), 100 U/ml penicillin, and 100 μg/ml streptomycin for 12 hours at 37°C; washed; and then incubated with the supernatant of degranulated BMCMCs (30 μl/ml final concentration) for 30 minutes at 37°C before assessment of contractility. To evaluate whether mast cell products were acting on epithelial cells, we completely removed epithelium in some rings by gentle rubbing with the airway brush. Epithelial removal was confirmed for each individual ring by microscopic observation of H&E-stained sections.

qRT-PCR. Total RNA was isolated with RNeasy kit (Qiagen). cDNA was analyzed by SYBR-Green real-time PCR with an ABI 7900HT thermocycler and normalized to *Gapdh* expression. Primers used were as follows: *Gapdh* forward, TGGTGAAGGTCGGTGTGAAC; *Gapdh* reverse, GACAAGCTTCCCATTCTCGG; *Cdh1* forward, CGTCCATGTGTGTGACTGTG; *Cdh1* reverse, GCTCTTTGACCACCGTTCTC; *Foxj1* forward, ACCAAGATCACTCTGTCGGC; *Foxj1* reverse, TGTTCAAGGACAGGTTGTGG; *Acta2* forward, TCCTGACGCTGAAGTATCCG; *Acta2* reverse, GTGCCTCTGTCAGCAGTGTC; *Pecam1* forward, CAAGCAAAGCAGTGAGCTG; *Pecam1* reverse, AGCAGGACAGGTCCAACAAC; *Mcpt1* forward, TTCCAGGTCTGTGTGGGAAG; *Mcpt1* reverse, TCCAGGGCACATATGCAGAG; *Mcpt2* forward, AACGGTTCGAAGGAGAGGTG; *Mcpt2* reverse, TCTGCTGTGTGGGTTCGTTC; *Mcpt4* forward, TCACCACTGAGAGAGGGTTCA; *Mcpt4* reverse, CATGAGCTCCAAGGGTGACA; *Cma1* forward, CCTGCAGTGGCTTCCTGATA; *Cma1* reverse, GCATGATGTCGTGGACAACC; *Tpsb2* forward,

GAGCTTGAGGTCCCTGTGAA; *Tpsb2* reverse, GATAAGGAGGTGGGAGAGGC; *Cpa3* forward, GACCAAACTCTTGGACCGGA; *Cpa3* reverse, GTTGAGGTCAGTGCCAATGC.

Western blotting. Lysates of differentiated BMCMCs (2 μg) or the supernatant of degranulated BMCMCs (20 μl) were separated by 12% SDS-PAGE, transferred to a polyvinylidene difluoride membrane (Millipore), and blocked for 30 minutes in Tris-buffered saline containing 5% skim milk. Membranes were incubated with antibodies to mMCP-1, mMCP-2, mMCP-4, or mMCP-6 for 1 hour, then with peroxidase-conjugated secondary antibody for 1 hour, and developed with Plus-ECL reagent (PerkinElmer). *Statistics*. Paired data were evaluated using a 2-tailed Student's *t* test. 1-way ANOVA was used for multiple comparisons, and when differences were statistically significant, this was followed with a *t* test with Bonferroni correction for subsequent pairwise analysis. Data were analyzed with StatView version 5.0 software. Differences with a *P* value less than 0.05 were considered statistically significant.

Study approval. All experiments were approved by the Institutional Animal Care and Use Committee of UCSF.

Acknowledgments

This work was supported by a NIH/NCRR UCSF-CTSI grant and NIH grants AI077439, HL53949, and HL102292 (to D. Sheppard); by Medical Research Council (to M Åbrink); by NIH grant HL024136 (to G. Caughey); and by the UCSF Strategic Asthma Basic Research (SABRE) Program. We thank Rebecca Barbeau, Chris Eisley, and Andrea Barczak (Functional Genomics Core, UCSF) for microarray analyses and Alan Pemberton for providing mMCP-1 and mMCP-2 antibodies.

Received for publication May 2, 2011, and accepted in revised form November 30, 2011.

Address correspondence to: Dean Sheppard, Box 2922, University of California, San Francisco, San Francisco, California 94143-3922, USA. Phone: 415.514.4269, Fax: 415.514.4278; E-mail: Dean.Sheppard@ucsf.edu.

1. Bradding P, Walls AF, Holgate ST. The role of the mast cell in the pathophysiology of asthma. *J Allergy Clin Immunol*. 2006;117(6):1277–1284.
2. Trivedi NN, Caughey GH. Mast cell peptidases: chameleons of innate immunity and host defense. *Am J Respir Cell Mol Biol*. 2010;42(3):257–267.
3. Amin K, Janson C, Boman G, Venge P. The extracellular deposition of mast cell products is increased in hypertrophic airways smooth muscles in allergic asthma but not in nonallergic asthma. *Allergy*. 2005;60(10):1241–1247.
4. Brightling CE, Bradding P, Symon FA, Holgate ST, Wardlaw AJ, Pavord ID. Mast-cell infiltration of airway smooth muscle in asthma. *N Engl J Med*. 2002;346(22):1699–1705.
5. Taube C, et al. Mast cells, Fc epsilon RI, and IL-13 are required for development of airway hyperresponsiveness after aerosolized allergen exposure in the absence of adjuvant. *J Immunol*. 2004; 172(10):6398–6406.
6. Yu M, Tsai M, Tam SY, Jones C, Zehnder J, Galli SJ. Mast cells can promote the development of multiple features of chronic asthma in mice. *J Clin Invest*. 2006;116(6):1633–1641.
7. Munger JS, et al. The integrin alpha v beta 6 binds and activates latent TGF beta 1: a mechanism for regulating pulmonary inflammation and fibrosis. *Cell*. 1999;96(3):319–328.
8. Horan GS, et al. Partial inhibition of integrin alpha(v)beta6 prevents pulmonary fibrosis without exacerbating inflammation. *Am J Respir Crit Care Med*. 2008;177(1):56–65.
9. Pittet JF, et al. TGF-beta is a critical mediator of acute lung injury. *J Clin Invest*. 2001;107(12):1537–1544.
10. Morris DG, et al. Loss of integrin alpha(v)beta6-mediated TGF-beta activation causes Mmp12-dependent emphysema. *Nature*. 2003;422(6928):169–173.
11. Li MO, Flavell RA. TGF-beta: a master of all T cell trades. *Cell*. 2008;134(3):392–404.
12. Li MO, Wan YY, Sanjabi S, Robertson AK, Flavell RA. Transforming growth factor-beta regulation of immune responses. *Annu Rev Immunol*. 2006; 24:99–146.
13. Gorelik L, Flavell RA. Transforming growth factor-beta in T-cell biology. *Nat Rev Immunol*. 2002;2(1):46–53.
14. Hetzel M, Bachem M, Anders D, Trischler G, Faehling M. Different effects of growth factors on proliferation and matrix production of normal and fibrotic human lung fibroblasts. *Lung*. 2005;183(4):225–237.
15. Hagimoto N, et al. TGF-beta 1 as an enhancer of Fas-mediated apoptosis of lung epithelial cells. *J Immunol*. 2002;168(12):6470–6478.
16. Kim KK, et al. Alveolar epithelial cell mesenchymal transition develops in vivo during pulmonary fibrosis and is regulated by the extracellular matrix. *Proc Natl Acad Sci U S A*. 2006;103(35):13180–13185.
17. Willis BC, Borok Z. TGF-beta-induced EMT: mechanisms and implications for fibrotic lung disease. *Am J Physiol Lung Cell Mol Physiol*. 2007;293(3):L525–L534.
18. Mangan PR, et al. Transforming growth factor-beta induces development of the T(H)17 lineage. *Nature*. 2006;441(7090):231–234.
19. Bettelli E, et al. Reciprocal developmental pathways for the generation of pathogenic effector TH17 and regulatory T cells. *Nature*. 2006;441(7090):235–238.
20. Chen W, et al. Conversion of peripheral CD4+CD25- naive T cells to CD4+CD25+ regulatory T cells by TGF-beta induction of transcription factor Foxp3. *J Exp Med*. 2003;198(12):1875–1886.
21. Nakao A, et al. Blockade of transforming growth factor beta/Smad signaling in T cells by overexpression of Smad7 enhances antigen-induced airway inflammation and airway reactivity. *J Exp Med*. 2000;192(2):151–158.
22. Moritz DR, Rodewald HR, Gheyselinck J, Klemenz R. The IL-1 receptor-related T1 antigen is expressed on immature and mature mast cells and on fetal blood mast cell progenitors. *J Immunol*. 1998; 161(9):4866–4874.
23. Pemberton AD, et al. Purification and characterization of mouse mast cell proteinase-2 and the differential expression and release of mouse mast cell proteinase-1 and -2 in vivo. *Clin Exp Allergy*. 2003;33(7):1005–1012.
24. Miller HR, Wright SH, Knight PA, Thornton EM. A novel function for transforming growth factor-beta1: upregulation of the expression and the IgE-independent extracellular release of a mucosal mast cell granule-specific beta-chymase, mouse mast cell protease-1. *Blood*. 1999;93(10):3473–3486.
25. Raymond WW, et al. Alpha 2-macroglobulin capture allows detection of mast cell chymase in serum and creates a reservoir of angiotensin II-generating activity. *J Immunol*. 2009;182(9):5770–5777.
26. Farghaly HS, Blagbrough IS, Medina-Tato DA, Watson ML. Interleukin 13 increases contractility of murine tracheal smooth muscle by a phosphoinositide 3-kinase p110delta-dependent mechanism. *Mol Pharmacol*. 2008;73(5):1530–1537.
27. Andersson MK, Karlson U, Hellman L. The extended cleavage specificity of the rodent beta-chymases rMCP-1 and mMCP-4 reveal major functional similarities to the human mast cell chymase. *Mol Immunol*. 2008;45(3):766–775.
28. Zuyderduyn S, Hiemstra PS, Rabe KF. TGF-beta differentially regulates TH2 cytokine-induced eotaxin and eotaxin-3 release by human airway smooth muscle cells. *J Allergy Clin Immunol*. 2004;114(4):791–798.
29. Knight PA, Brown JK, Wright SH, Thornton EM, Pate JA, Miller HR. Aberrant mucosal mast cell protease expression in the enteric epithelium of nematode-infected mice lacking the integrin alphavbeta6, a transforming growth factor-beta1 activator. *Am J Pathol*. 2007;171(4):1237–1248.
30. Gruber BL, Marchese MJ, Kew RR. Transforming growth factor-beta 1 mediates mast cell chemotaxis. *J Immunol*. 1994;152(12):5860–5867.
31. Olsson N, Piek E, Sundstrom M, ten Dijke P, Nilsson G. Transforming growth factor-beta-mediated mast cell migration depends on mitogen-activated protein kinase activity. *Cell Signal*. 2001;13(7):483–490.
32. Rosbottom A, Scudamore CL, von der Mark H, Thornton EM, Wright SH, Miller HR. TGF-beta 1 regulates adhesion of mucosal mast cell homologues to laminin-1 through expression of integrin alpha 7. *J Immunol*. 2002;169(10):5689–5695.
33. Brown JK, et al. Expression of integrin-alphaE by mucosal mast cells in the intestinal epithelium and its absence in nematode-infected mice lacking the transforming growth factor-beta1-activating integrin alphavbeta6. *Am J Pathol*. 2004;165(1):95–106.
34. Gomez G, et al. TGF-beta 1 inhibits mast cell Fc epsilon RI expression. *J Immunol*. 2005; 174(10):5987–5993.
35. Knight PA, Wright SH, Brown JK, Huang X, Sheppard D, Miller HR. Enteric expression of the integrin alpha(v)beta(6) is essential for nematode-induced mucosal mast cell hyperplasia and expression of the granule chymase, mouse mast cell protease-1. *Am J Pathol*. 2002;161(3):771–779.
36. Abonia JP, et al. Alpha-4 integrins and VCAM-1, but not MAdCAM-1, are essential for recruitment of mast cell progenitors to the inflamed lung. *Blood*. 2006;108(5):1588–1594.
37. Huang XZ, et al. Inactivation of the integrin beta 6 subunit gene reveals a role of epithelial integrins in regulating inflammation in the lung and skin. *J Cell Biol*. 1996;133(4):921–928.
38. Williams CM, Galli SJ. Mast cells can amplify airway reactivity and features of chronic inflammation in an asthma model in mice. *J Exp Med*. 2000;192(3):455–462.
39. Okayama Y, Ra C, Saito H. Role of mast cells in airway remodeling. *Curr Opin Immunol*. 2007; 19(6):687–693.
40. Waern I, et al. Mouse mast cell protease 4 is the major chymase in murine airways and has a protective role in allergic airway inflammation. *J Immunol*. 2009;183(10):6369–6376.
41. Dougherty RH, et al. Accumulation of intraepithelial mast cells with a unique protease phenotype in T(H)2-high asthma. *J Allergy Clin Immunol*.

2010;125(5):1046–1053.
42. Balzar S, Chu HW, Strand M, Wenzel S. Relationship of small airway chymase-positive mast cells and lung function in severe asthma. *Am J Respir Crit Care Med*. 2005;171(5):431–439.
43. Andersson MK, Pemberton AD, Miller HR, Hellman L. Extended cleavage specificity of mMCP-1, the major mucosal mast cell protease in mouse-high specificity indicates high substrate selectivity. *Mol Immunol*. 2008;45(9):2548–2558.
44. Coussens LM, et al. Inflammatory mast cells upregulate angiogenesis during squamous epithelial carcinogenesis. *Genes Dev*. 1999;13(11):1382–1397.
45. Raymond WW, Cruz AC, Caughey GH. Mast cell and neutrophil peptidases attack an inactivation segment in hepatocyte growth factor to generate NK4-like antagonists. *J Biol Chem*. 2006;281(3):1489–1494.
46. Tchougounova E, Lundequist A, Fajardo I, Winberg JO, Abrink M, Pejler G. A key role for mast cell chymase in the activation of pro-matrix metalloprotease-9 and pro-matrix metalloprotease-2. *J Biol Chem*. 2005;280(10):9291–9296.
47. Scudamore CL, McMillan L, Thornton EM, Wright SH, Newlands GF, Miller HR. Mast cell heterogeneity in the gastrointestinal tract: variable expression of mouse mast cell protease-1 (mMCP-1) in intraepithelial mucosal mast cells in nematode-infected and normal BALB/c mice. *Am J Pathol*. 1997;150(5):1661–1672.
48. Caughey GH, Raymond WW, Wolters PJ. Angiotensin II generation by mast cell alpha- and beta-chymases. *Biochim Biophys Acta*. 2000;1480(1–2):245–257.
49. Tchougounova E, Pejler G, Abrink M. The chymase, mouse mast cell protease 4, constitutes the major chymotrypsin-like activity in peritoneum and ear tissue. A role for mouse mast cell protease 4 in thrombin regulation and fibronectin turnover. *J Exp Med*. 2003;198(3):423–431.
50. Chen C, Huang X, Sheppard D. ADAM33 is not essential for growth and development and does not modulate allergic asthma in mice. *Mol Cell Biol*. 2006;26(18):6950–6956.
51. Pemberton AD, Brown JK, Wright SH, Knight PA, Miller HR. The proteome of mouse mucosal mast cell homologues: the role of transforming growth factor beta1. *Proteomics*. 2006;6(2):623–631.
52. Fifadara NH, Aye CC, Raghuwanshi SK, Richardson RM, Ono SJ. CCR1 expression and signal transduction by murine BMMC results in secretion of TNF-alpha, TGFbeta-1 and IL-6. *Int Immunol*. 2009;21(8):991–1001.

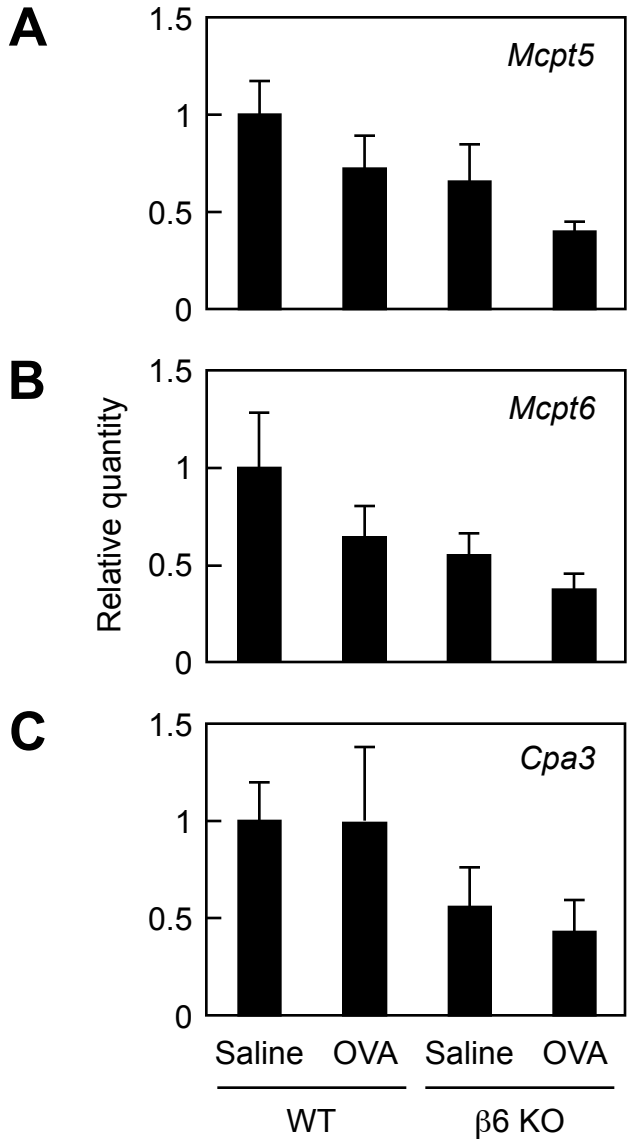

Supplementary Figure 1 Expression profiles of mast cell protease transcripts in whole lung from chronically OVA challenged WT or β6 KO mice. Total RNA isolated from whole lung from WT or β6 KO mice was analyzed for (A) *Mcpt5*, (B) *Mcpt6* and (C) *Cpa3* expression by qRT-PCR. Values for each mRNA were normalized to GAPDH and relative quantity was calculated relative to expression in saline treated WT mice. Data are mean ± SEM for 3 independent samples.

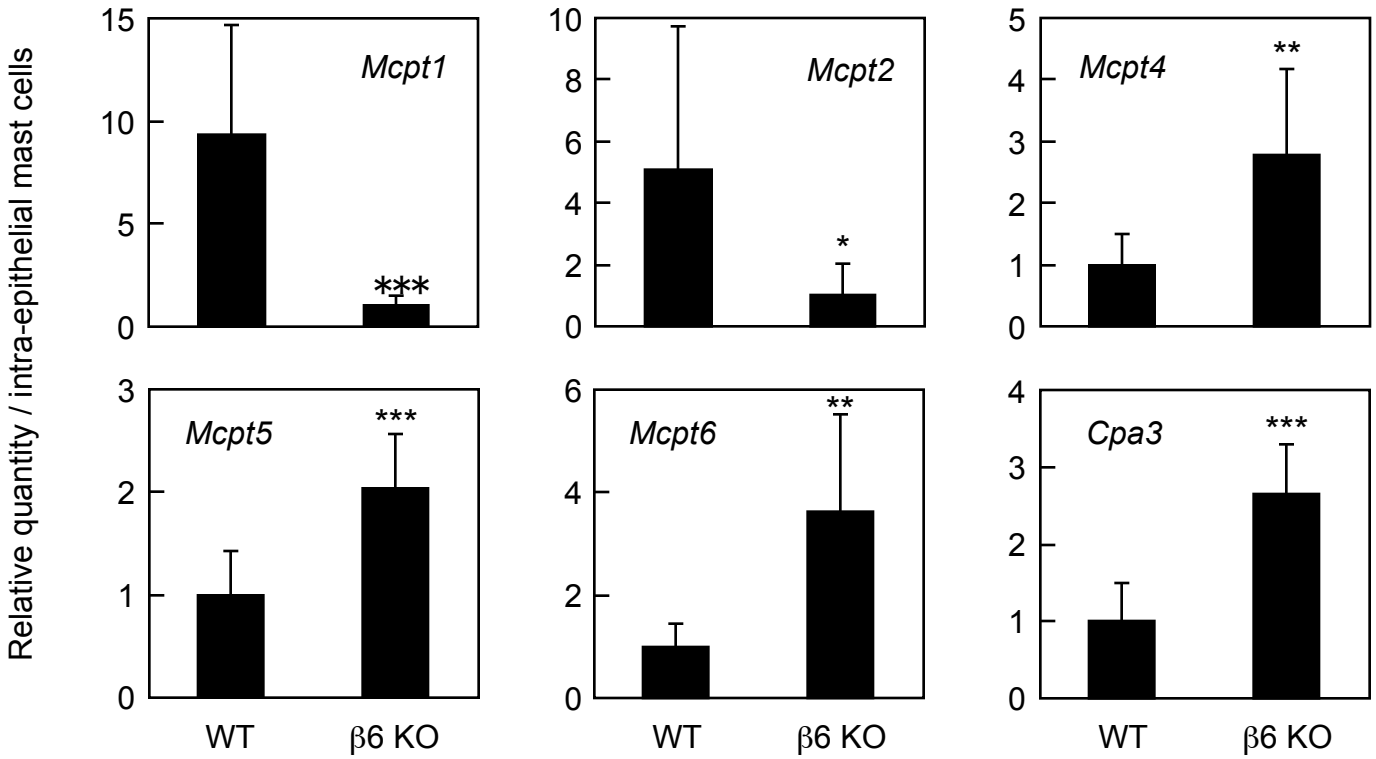

Supplementary Figure 2 Expression profiles of mast cell protease transcripts in brushing samples from untreated wt and β6 KO mice after normalization to number of intra-epithelial mast cells. Values for each mRNA were normalized to GAPDH. The relative quantity for *Mcpt1 and 2* was calculated relative to expression in β6 KO samples and for *Mcpt4, 5, 6 and Cpa3* was calculated relative to expression in WT samples. Data are mean ± SEM for 8 independent samples. **P* <0.05, ***P* <0.01, ****P* <0.001 compared with untreated WT mice

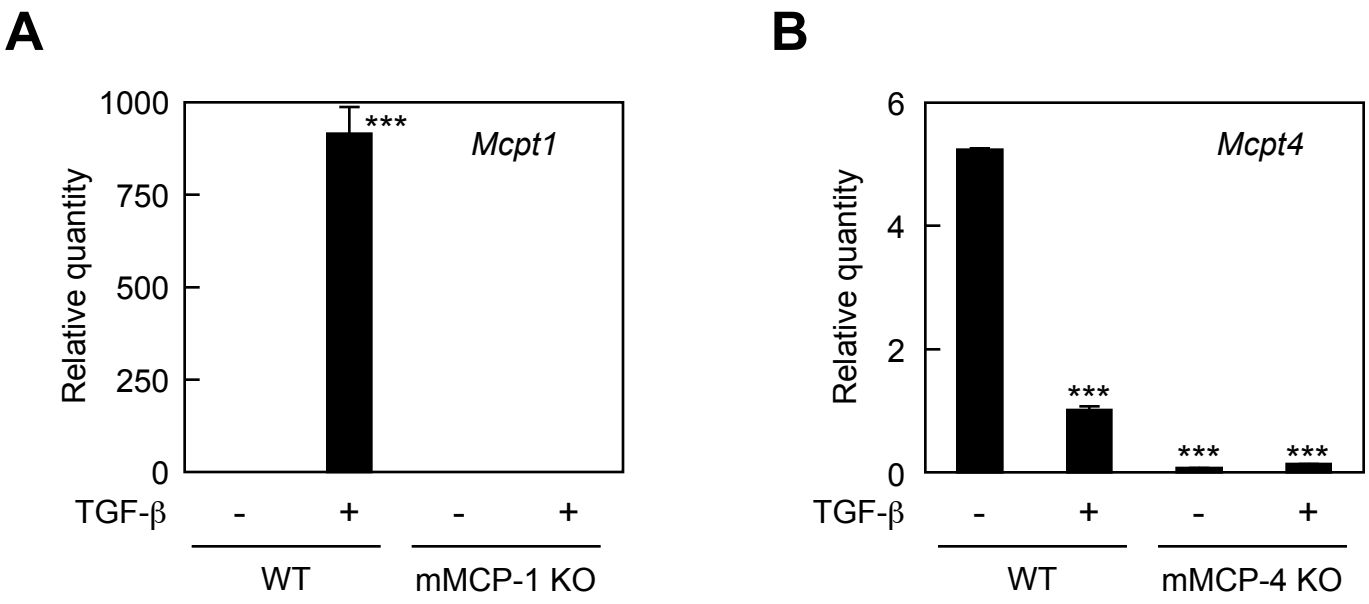

Supplementary Figure 3 mMCP-1 KO and mMCP-4 KO mice have complete deletion of mMCP-1 and mMCP-4 expression in BMCMCs. *In vitro* differentiated BMCMCs from (A) mMCP-1 KO mice or (B) mMCP-4 KO mice were analyzed for *Mcpt1* and *Mcpt4* expression by qRT-PCR. Values for each mRNA were normalized to GAPDH. The relative quantity for *Mcpt1* was calculated relative to expression in TGF-β (-) samples and for *Mcpt4* was calculated relative to expression in TGF-β (+) samples. Data are mean ± SEM for 3 independent samples. ***P <0.001 compared with WT TGF-β(-).

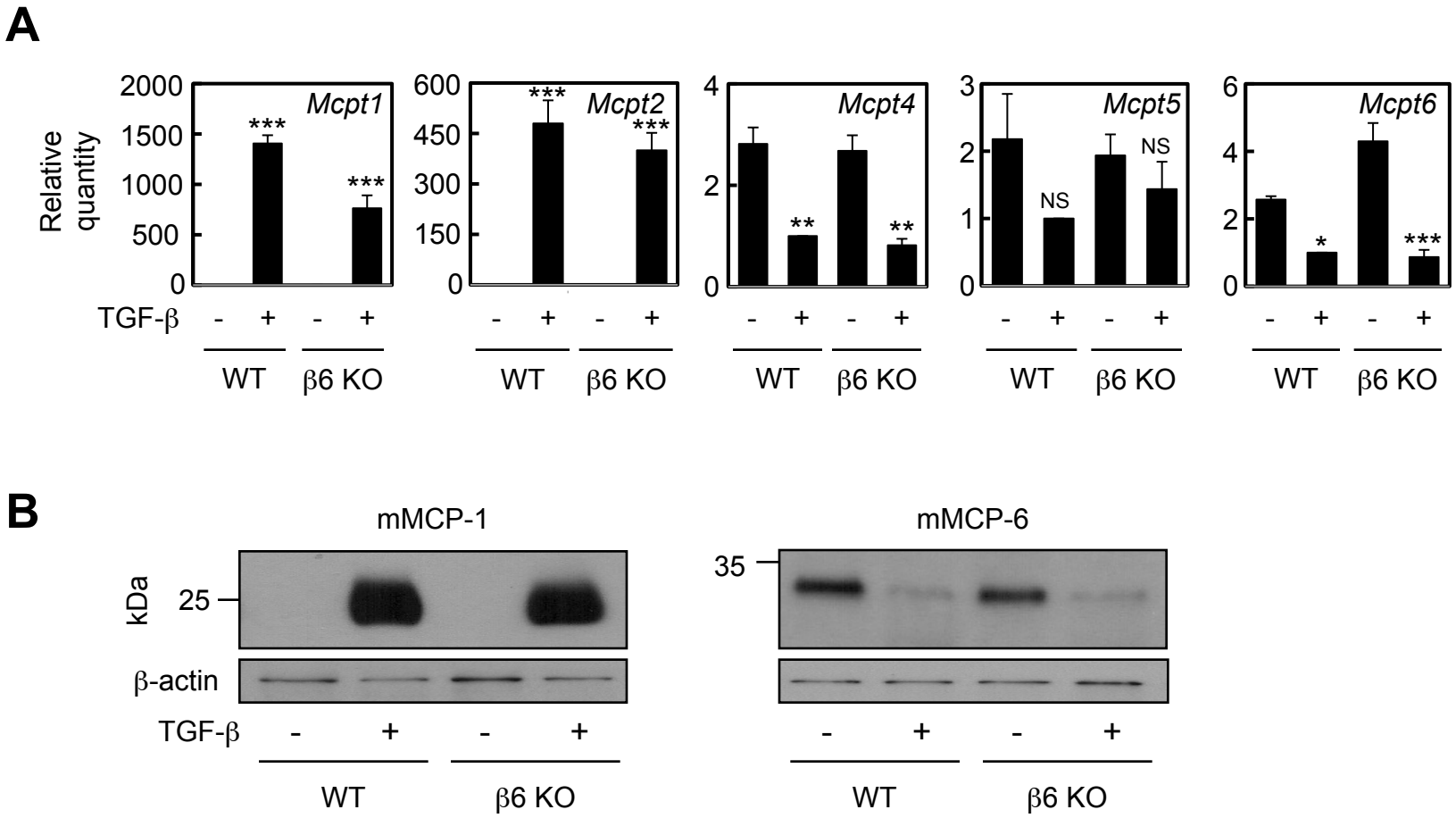

Supplementary Figure 4 BMCMCs from WT and β6 KO mice respond similarly to stimulation with TGF-β. (A) Expression profiles of mast cell protease transcripts by qRT-PCR from WT and β6 KO mice differentiated in the presence or absence of TGF-β for 3 weeks. mRNA concentrations were normalized to GAPDH. The relative quantity for *Mcpt1 and 2* was calculated relative to expression in WT TGF-β (-) samples and for *Mcpt4, 5 and 6* was calculated relative to expression in WT TGF-β (+) samples. Data are mean ± SEM for 3 independent samples. *P <0.05, **P <0.01, ***P <0.001 compared with TGF-β untreated samples. (B) Western blot analysis of mast cell proteases in 2 μg of protein from cell lysates of cultured BMCMCs from WT and β6 KO mice differentiated in the presence or absence of TGF-β. β-actin was used as a control for equal protein loading.

Supplementary Table 1 Genes most increased at baseline in β6 knockout epithelium

Agilent probe ID	Symbol	Description	Fold increase*
A_51_P514035	*Cma1* (*Mcpt5*)	Mast cell chymase 1 (Mast cell protease 5)	14.3
A_51_P514029	*Cma1* (*Mcpt5*)	Mast cell chymase 1 (Mast cell protease 5)	13.1
A_51_P145130	*Mcpt4*	Mast cell protease 4	13.0
A_51_P214127	*Cpa3*	Carboxypeptidase A3, mast cell	12.6
A_52_P254155	*Mcpt6* (*Tpsb2*)	Mast cell protease 6	11.0
A_51_P145132	*Mcpt4*	Mast cell protease 4	8.6
A_52_P8459	*Tpsab1* (*Mcpt7*)	Tryptase α/β1 (Mast cell protease 7)	8.2
A_52_P484194	*Il1rl1*	Interleukin 1 receptor-like 1 (Interleukin 33 receptor)	7.2
A_51_P258721	*Tpsg1*	Tryptase γ1	6.3
A_51_P429770	*Fcer1a*	Fc receptor, IgE, high affinity I, α polypeptide	5.3

* Values represent fold increase with significant (adjusted $P < 0.01$) changes in epithelium of β6 KO mice compared to WT mice.

Supplementary Table 2 Genes most induced by OVA in WT mice

Agilent probe ID	Symbol	Description	Fold increase		Adjusted *p* WT OVA vs. β6 KO OVA
			WT *	β6 KO **	
A_51_P335460	*Clca3*	Chloride channel calcium activated 3	36.5	36.8	NS
A_51_P335460	*Scin*	Scinderin	22.4	11.4	NS
A_51_P169476	*Mcpt1*	Mast cell protease 1	18.2	1.9	< 0.05
A_51_P147987	*Itln*	Intelectin	9.2	13.6	NS
A_51_P434567	*Adra2a*	Adrenergic receptor, α2a	9.0	4.1	NS
A_52_P379474	ENSMUST00000043170	Unknown	8.9	12.5	NS
A_52_P67493	*Adra2a*	Adrenergic receptor, α2a	8.7	4.5	NS
A_51_P173114	*Pcdh21*	Protocadherin 21	6.7	3.4	NS

* Values represent fold increase with significant (adjusted $P < 0.01$) changes in epithelium from OVA-treated WT mice compared to saline-treated WT mice.

** Values represent fold increase in epithelium from OVA-treated β6 KO mice compared to saline-treated β6 KO mice.